

Biodegradation of Phenol Using *Bacillus cereus* WJ1 and Evaluation of Degradation Efficiency Based on a Graphene-Modified Electrode

Yan Zhang¹, Daban Lu¹, Tianzhen Ju², Letao Wang¹, Shaoxiong Lin¹, Yue Zhao², Chunming Wang^{1,*}, Haijing He¹, Yongling Du¹

¹ Department of Chemistry, Lanzhou University, Lanzhou 730000, P. R. China

² Department of College of Geography and Environment Science, Northwest Normal University, Lanzhou 730070, P. R. China

*E-mail: wangcm@lzu.edu.cn

Received: 10 October 2012 / Accepted: 25 November 2012 / Published: 1 January 2013

A bacterial strain was isolated from the phenol-contaminated wastewater, and was identified as a member of *Bacillus cereus* based on standard morphological, biochemical characteristics and 16S rDNA sequence analysis. The strain exhibited optimum phenol degradation performance with the addition of 100 mg/L glucose at pH 7.0, 30 °C. Haldane's model could be fitted to the growth kinetics data well over a range of initial phenol concentrations (50-600 mg/L), with kinetic values maximum specific growth rates $\mu_{\max} = 0.153 \text{ h}^{-1}$, half saturation coefficient $K_s = 21.33 \text{ mg/L}$ and substrate inhibition coefficient $K_i = 238 \text{ mg/L}$. The concentration of phenol was determined using differential pulse voltammetry (DPV) at graphene (GR)-modified glassy carbon electrode (GCE) in the presence of cetyltrimethylammonium bromide (CTAB). Under the optimized conditions, the oxidation peak current of phenol was linear over a concentration range from 0.05 to 100 mg/L with the detection limit (S/N =3) of 0.02 mg/L. This method combined phenol biodegradation with electrochemical determination, and the results were satisfactory.

Keywords: Biodegradation; Phenol; Differential pulse voltammetry; Graphene; Cetyltrimethylammonium bromide

1. INTRODUCTION

Phenolic products are toxic to humans and aquatic organisms, which can be found in several types of industrial wastewater, such as the wastewater from oil refineries, phenol manufacturing pharmaceuticals, industries of resins, paints, dyes, petrochemicals, textiles and paper mills [1, 2]. Phenol is toxic upon ingestion, contact or inhalation and it is recommended that human exposure to

phenol should not exceed 20 mg in an average day. Also, phenol can be lethal in fish at concentrations of 5-25 ppm [2, 3]. So, it's necessary to develop highly efficient techniques to remove these pollutants from the wastewater for environmental protection.

Compared with traditional physical and chemical methods, biological degradation technique is a promising method because of its effectiveness, lower costs and innocuous end products. In biodegradation of toxic chemicals, the microorganisms play a critical role. In spite of the toxicity of phenol, a number of microorganisms have been reported to degrade phenol, including *Candida tropicalis*, *Bacillus brevis*, *Corynebacterium* sp., *Bacillus amyloliquefaciens*, *Gliomastix indicus* and *Pseudomonas putida* [4-9]. Additionally, the determination of phenol concentration is still a subject of intense concern and various approaches have been devised, such as gas chromatography [10], high-pressure liquid chromatography (HPLC) [11], spectrophotometry [12], biosensor-based method [13], capillary electrophoretic method [14] and electrochemical method [15]. In contrast to these methods, electrochemical technique has attracted considerable attention due to its simpleness, convenience and low cost. For the investigation of phenol concentration, glassy carbon electrode (GCE) is most commonly employed as the working electrode because it shows high stability and preciseness in detection. Furthermore, the modified electrode shows obvious electrocatalytic activity towards the oxidation of phenol. In present work, graphene (GR) modified GCE was fabricated in the presence of a long-chain cationic surfactant cetyltrimethylammonium bromide (CTAB) and its applications for phenol determination were investigated. Graphene is a single layer of carbon atoms in a closely packed honeycomb two-dimensional lattice. Because of its large surface and high conductivity, graphene shows potential application in chemically modified electrodes (CMEs), and some investigations about the aspect have been reported [16-18]. Surfactants are a kind of amphiphilic molecules, which are capable of changing the electrical properties of the electrode solution interface and the electrochemical process through adsorption at interfaces or aggregation into supramolecular structures [19].

In this study, phenol degraded by a newly isolated *Bacillus*, which was named after *Bacillus cereus* WJ1, was described. The effects of the various abiotic factors, such as pH value, temperature and glucose concentration on the biodegradation performance of phenol by strain WJ1, were evaluated. The growth and phenol degradation kinetics of this strain were examined in batch experiments. Herein, differential pulse voltammetry (DPV) was used to measure the concentration of phenol using GR-modified GCE in the presence of CTAB for greatly enhancing the sensitivity and stability of electrochemical measurements of phenol.

2. EXPERIMENTAL

2.1. Reagents

Graphene (GR) was synthesized through chemically reducing graphite oxide which was synthesized from graphite by the modified Hummers method [20]. All chemicals used for culturing of microorganisms were purchased from Beijing Shuangxuan Microbe Culture Medium Products Factory. Phenol and Cetyltrimethylammonium bromide (CTAB) were obtained from Beijing Chemical Factory.

All other reagents and solvents were of analytical grade and used without further purification. All chemicals were prepared with deionized water purified via Milli-Q unit.

2.2. Isolation of the microorganism

The bacteria were isolated by the enrichment culture technique at 30 °C from a phenol-contaminated wastewater sample from Jiuquan industrial effluents in Gansu province, China. Phenol-containing mineral salt medium was used for the isolation of bacteria. The mineral salt medium (MSM) was composed of 0.5 g/L KH_2PO_4 , 0.5 g/L K_2HPO_4 , 0.2 g/L $\text{MgSO}_4 \cdot 7\text{H}_2\text{O}$, 0.1 g/L CaCl_2 , 0.2 g/L NaCl , 1.0 g/L NH_4NO_3 , 0.01 g/L $\text{MnSO}_4 \cdot \text{H}_2\text{O}$, 0.01 g/L $\text{Fe}_2(\text{SO}_4)_3 \cdot 3\text{H}_2\text{O}$, the pH of the media was adjusted to 7.0 with NaOH or HCl solution. All media and Erlenmeyer flasks fitted with cotton plugs were autoclaved at 121 °C for 20 min for sterilization before use. 5 mL of the industrial effluents was added to 50 mL MSM containing 100 mg/L phenol in 250 mL Erlenmeyer flasks. The samples were incubated at 30 °C for 48 h in a rotary shaker with a speed of 150 rpm. When the phenol depleted, 5 mL of the cultures were transferred to fresh MSM to initiate the degradation. From then on, phenol concentration increased stepwise, varying from 100 mg/L to final 600 mg/L at 100 mg/L interval. After six transfers of consecutive enrichments had been carried out, dilutions of culture were inoculated on MSM agar plates incubated at 30 °C for 24 h. Agar plates contained 20 g of agar per liter of medium. Then the predominant colonies were transferred to fresh MSM agar plates two times to ensure culture purity. Each isolate was then tested for its ability to degradation phenol at 300 mg/L. One of the isolates obtained exhibited the best ability of degrading phenol and was selected for further degradation study.

2.3. Characterization and identification of the strain

The bacterial isolate was examined by using cell morphology, gram reaction as well as standard physiological and biochemical tests. The morphological investigation was prepared using a DMBA200 optical microscope and scanning electron microscopy (SEM, JSM-5600LV, JEOL, Japan). The DNA extracts from bacterial isolate were amplified by PCR with primers 27F (5'-AGAGTTTGATCCTGGCTCAG-3') and 1492R (5'-GGTTACCTTGTTACGAC TT-3'). The reaction was carried out in a 50 μL volume, containing 10 \times PCR buffer (5 μL), 2 mM dNTP mixture (2.5 μL), 2 μL each of primers, Taq DNA polymerase (1 μL), dH_2O (up to 50 μL), template DNA (1 μL). The PCR amplification was performed as following conditions: predenaturation at 94 °C for 5 min, 36 cycles of denaturation at 94 °C for 1 min, annealing at 55 °C for 1 min and extension at 72 °C for 2 min, and finally extension at 72 °C for 10 min. After the PCR reaction, 5 μL of PCR products were also examined by electrophoresis. The 16S rDNA gene sequence was determined directly by Shanghai Bio. Tech. Company. The sequences obtained were compiled and compared with sequences in the GenBank databases using BLAST program. A maximum likelihood phylogenetic tree was generated by neighbor-joining methods.

2.4. Biodegradation experiments

The biodegradation experiments were carried out in a series of 250 mL Erlenmeyer flasks containing 50 mL sterile MSM. To investigate the phenol biodegradation performance at different pH value, temperature and glucose concentration, strain WJ1 was transferred into flasks with an initial biomass concentration of 30 mg/L and initial phenol concentration of 300 mg/L. In order to find out the optimum initial phenol concentration for the growth of the bacteria and analyze their growth kinetics, additional experiments were carried out with various initial phenol concentrations ranging from 50 to 600 mg/L. Control flasks without bacteria were incubated in parallel under the same conditions to ascertain the evaporation loss of phenol. All the flasks were sealed with cotton stoppers and shaken in a rotary shaker with a speed of 150 rpm. Samples of the flasks were separately taken at appropriate times to observe phenol removal and cell density.

2.5. Phenol biodegradation kinetics

The growth rate of biomass in a batch system can be modeled by the following equation:

$$\frac{dX}{dt} = \mu X - k_d X \quad (1)$$

where X is the biomass concentration (mg/L), μ is the specific growth rate of the biomass (h^{-1}), k_d is the endogenous coefficient (h^{-1}).

Moreover, during exponential phase, endogenous coefficient k_d in Eq. (1) may be neglected. Eq. (1) therefore reduces to the following equation:

$$\frac{dX}{dt} = \mu X \quad (2)$$

In the exponential phase, the specific growth rate is calculated by:

$$\mu = \frac{\ln(X_2 / X_1)}{t_2 - t_1} \quad (3)$$

The kinetics of phenol biodegradation by microbial populations has been extensively investigated. Of the kinetics models describing the growth kinetics with an inhibitory compound, the Haldane model has frequently been used [4, 8]. The Haldane equation is as follows:

$$\mu = \frac{\mu_{\max} S}{K_s + S + S^2 / K_i} \quad (4)$$

where S is the substrate concentration (mg/L), μ_{\max} is the maximum specific growth rate (h^{-1}), K_s is the half saturation coefficient (mg/L) and K_i is the inhibition coefficient (mg/L).

The yield coefficient for phenol can be calculated by the following equation:

$$Y = \frac{X_{\max} - X_0}{S_0 - S_s} \quad (5)$$

where X_{\max} is the maximum dry cell concentration (mg/L), X_0 is the initial dry cell concentration (mg/L), S_0 is the initial phenol concentration (mg/L) and S_s is the substrate concentration when cell concentration reached maximum (mg/L).

2.6. Analytical methods

Cell concentration was determined from optical density (OD) measurements at 600 nm using an UV/visible spectrophotometer (752N, Shanghai, China) with the culture medium as reference. The samples exceeding 0.8 OD were appropriately diluted with the culture medium so that the Beer-Lambert law was applied for the determination of biomass concentration [8]. The biomass dry-weight concentrations were measured by centrifuging the cell suspension at 10000 rpm for 10 min and drying the cells to a constant weight at 105 °C for 24 h. The surface of the modified electrode was characterized using scanning electron microscopy (SEM, JSM-5600LV, JEOL, Japan). The transmission electron microscope (TEM) image was obtained at JEOL-1200 EX TEM (Japan).

The concentration of phenol was measured at certain degradation intervals using DPV. Electrochemical experiments were performed with a CHI 1210A electrochemical workstation (CHI Instrument, China). A conventional three-electrode system, including a GR/GCE ($\Phi=3$ mm) working electrode, an Ag/AgCl reference electrode and a Pt wire counter-electrode, was employed. Before electrochemical measurements, the working electrode was polished with 0.05 μm γ -alumina, then cleaned ultrasonically in doubly distilled water for 2 min and finally cleaned in turn in an ultrasonic cleaner with 1:1 nitric acid solution, alcohol and doubly distilled water. 0.5 mg graphene was dispersed in 1 mL DMF by 20 min ultrasonic agitation to achieve a 0.5 mg/mL concentration. 8 μL of the suspension was cast on the surface of cleaned GCE and then the solvent DMF was evaporated in air to obtain a GR/GCE. After 300 s accumulation under open circuit potential, cyclic voltammograms (CVs) were performed in the potential range from 0 to 1.0 V at a scan rate of 100 mV/s. The parameters performed with DPV were chosen as follows: increment potential (V) = 0.004, amplitude (V) = 0.05, pulse width (s) = 0.05, pulse period (s) = 0.2. All experiments data chosen for electrochemical method were repeated in three times determination.

3. RESULTS AND DISCUSSION

3.1. Microorganism identification

After isolated by the enrichment culture technique, the bacterial strain was examined based on its morphological, physiological and biochemical characteristics as the genus *Bacillus*. The results of

physiological and biochemical tests of *Bacillus cereus* WJ1 are shown in Table 1. The SEM image reveals that the isolated strain is a rod shaped *bacillus* with approximate 1 μm in width and 2-4 μm in length (Figure 1). The partial 16S rDNA sequence analysis of isolate was determined. The sequence of strain WJ1 obtained by sequencing was found to be 1436 bp and was submitted to the GenBank database under accession no. HQ704377. Preliminary comparison of the sequence against the GenBank databases indicates that the members of the genus *Bacillus cereus* are its closest phylogenetic neighbors. The neighbor-joining tree is shown in Figure 2. Therefore, the isolate is designated as *Bacillus cereus* WJ1.

Table 1. Physiological and biochemical characteristics of *Bacillus cereus* WJ1 (+: positive; -: negative).

Analytical tests	Results
Morphology:	
Form	Rods
Size (μm)	2-4
Configuration	Round
Margin	Entire
Elevation	Raised
Surface	Flat
Pigment	Cream
Opacity	Opaque
Gram's stain	Gram positive
Spore	+
Motility	Motile
Physiological tests:	
Tolerance to NaCl (%)	Up to 8%
Growth temperature ($^{\circ}\text{C}$)	20-40
pH range of growth	5.0-10.0
Biochemical analysis:	
Starch hydrolysis	+
Gelatin hydrolysis	+
Oxidase test	+
Catalase test	+
Lecithinase test	+
Lysozyme test	+
Ammonia production	+
Indole test	+
MR (metylred) test	-
Voges-Proskauere test	+
Nitrate reduction	+
Citrate utilization	-
Hydrogen sulfide production	-
Phenylalanine deaminase	-
Acid production from:	
Xylose	-
Mannitol	-
Glucose	+

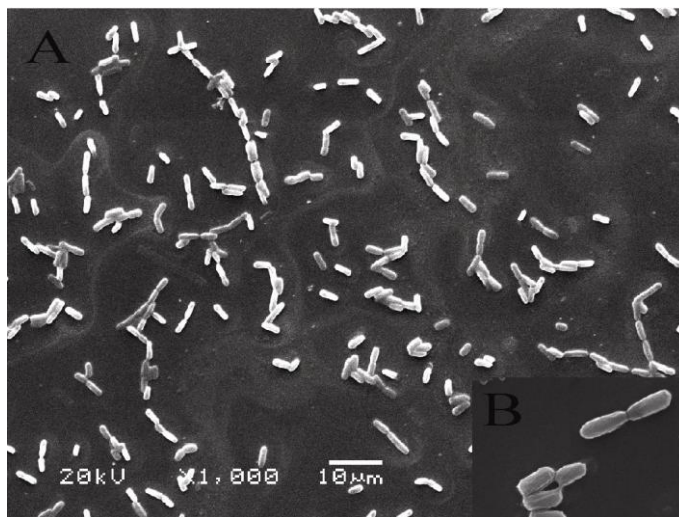


Figure 1. SEM images of WJ1 at 1000 \times magnification (A), 10000 \times magnification (B).

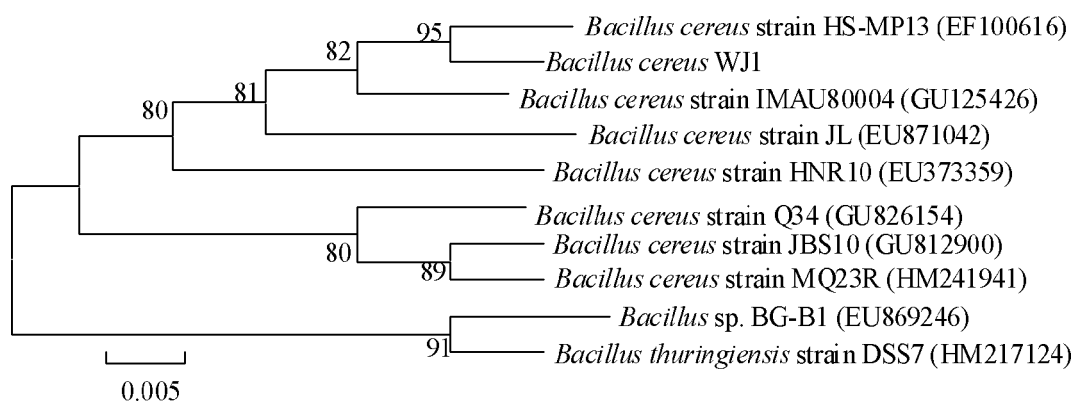


Figure 2. The neighbor-joining tree was constructed and bootstrapped (1000 iterations) to represent the relationship between the phenol-degrading strain WJ1 and representative species of the genus *Bacillus* and related genera. Bootstrap values are noted on the branch and the scale bar ($=0.005$) represents nucleotide substitution per 100 nucleotide.

3.2. Characterization of graphene and modified electrode

The morphologies of graphene were examined by the TEM and SEM studies. Figure 3A shows the TEM images of graphene nanosheets, clearly illustrating the flake-like shapes. The inset of Figure 3A is the selected-area electron diffraction (SAED) of graphene yielding a double six-spot-ring pattern, which confirms the benzene-ring pattern of the graphene sheet. Figure 3B shows the SEM image of graphene film on the surface of the GCE. It can be seen that a crumpled, wrinkled and layered structure of graphene sheet film is formed on the surface of GCE. This wrinkled nature of graphene is highly beneficial in maintaining a high surface area on the electrode since the sheets cannot readily collapse back to a graphitic structure [21, 22].

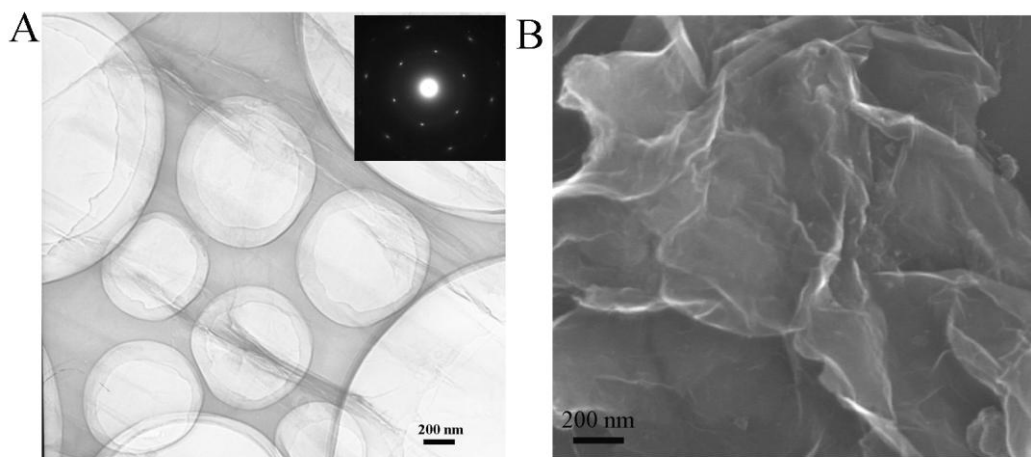


Figure 3. The TEM image of graphene (A), Inset: SAED pattern of graphene, and SEM image of graphene /GCE (B)

3.3. Electrochemical behavior of phenol

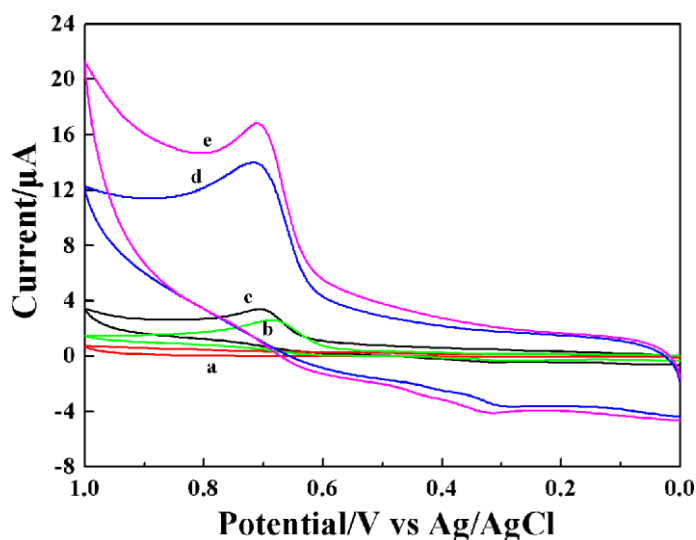


Figure 4. Cyclic voltammograms of bare GCE in 0.1 mol/L phosphate buffer (pH 7.0) (a) and 10 mg/L phenol at bare GCE (b), bare GCE in the presence of 1.0×10^{-4} mol/L CTAB (c), GR modified GCE in absence (d) and presence (e) of 1.0×10^{-4} mol/L CTAB. Scan rate: 100 mV/s; GR concentration: 0.5 mg/mL; amount of GR: 8 μ L.

The electrochemical behavior of phenol was investigated by cyclic voltammetry. As can be seen in Figure 4(a), no redox peaks are observed at bare GCE in blank PBS. At the bare GCE, phenol exhibits an irreversible behavior with a relatively weak oxidation peak (curve b). The oxidation peak current of phenol increased when 1.0×10^{-4} mol/L CTAB was added into the solution (curve c), indicating that CTAB could promote the oxidation of phenol. That is the surfactant can be adsorbed on solid-liquid interface to form surfactant film [17], which may result in the change in the overvoltage of the electrode and influence the rate of electron transfer. Here, the surfactant film of cationic surfactant

CTAB is hydrophilic and positively charged, while hydroxyl group in phenol is partially ionized and charged negatively. Thus, phenol can be accumulated on the electrode surface via electrostatic interaction with the adsorbed CTAB film, leading to the increase of the surface concentration of phenol and the increase of oxidation current. From curve (d) and (e), it can be seen that the oxidation peak current of GR-modified GCE increased greatly and the background current is larger than that of bare GCE and CTAB/GCE, which can be attributed to the large specific area and good conductivity of graphene [23]. Owing to the high quality of the sp^2 conjugated bond in the carbon lattice, graphene is highly conductive and shows metallic conductance even in the limit of zero carrier density [24]. So, it's feasible for the electron transfer because of the π - π interaction between phenyl structure of phenol and two-dimensional planar hexagonal carbon structure of graphene. Moreover, the adsorption of CTAB on GR/GCE which has a rather rough surface might form a uniform CTAB layer, which coupled with the possible reorientation of phenol in CTAB film might result in the uniformizing of the existing state of phenol on the electrode surface and be responsible for the increasing of the oxidation peak [25]. This is important for achieving high sensitivity and a low detection limit.

3.4. Optimization of electrochemical experimental parameters

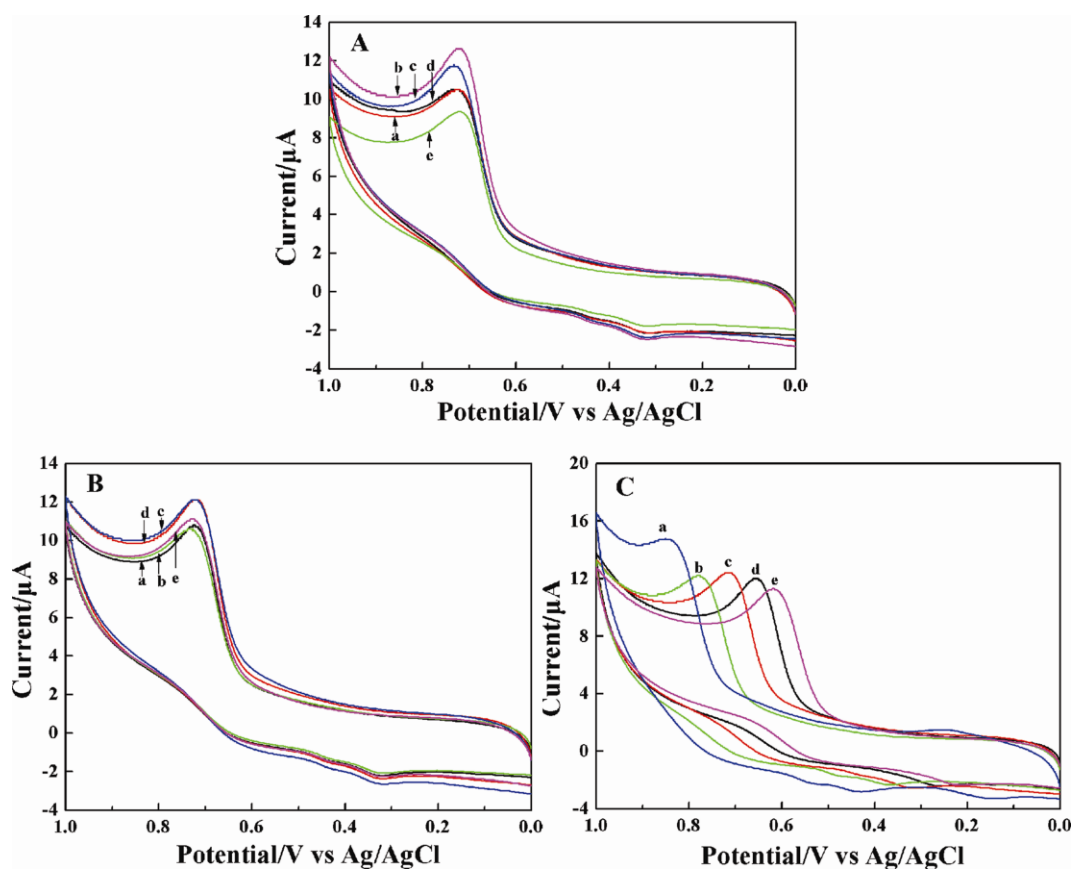


Figure 5. (A) Effect of amount of graphene at the electrode surface on the peak currents of 10 mg/L phenol in 0.1 mol/L phosphate buffer (pH 7.0): (a) 6 μ L (b) 8 μ L (c) 10 μ L (d) 12 μ L (e) 14 μ L. (B) Effect of concentration of CTAB: (a) 1.0×10^{-4} mol/L (b) 1.1×10^{-4} mol/L (c) 1.2×10^{-4} mol/L (d) 1.3×10^{-4} mol/L (e) 1.4×10^{-4} mol/L. (C) Effect of pH: (a) pH 5.0 (b) pH 6.0 (c) pH 7.0 (d) pH 8.0 (e) pH 9.0. CV conditions were same as Figure 4.

The effect of amount of GR-modified on the GCE surface on the oxidation peak current of phenol was investigated. As shown in Figure 5A, the current increases with increasing amount of GR on the electrode and reaches the maximum at 8 μL , then decreases significantly when the amount of GR increased further, which could be attributed to the increase of film thickness, leading to an increase of interface electron transfer resistance, making the electron transfer more difficult [23]. Therefore, 8 μL GR immobilized on the electrode was chosen for all subsequent experiments.

As shown in Figure 5B, the effect of CTAB concentration on the oxidation peak current of phenol was also investigated by cyclic voltammetry. The peak current increases gradually with the increase of CTAB concentration to 1.3×10^{-4} mol/L. Due to the micellar effect of surfactant, further increase of CTAB concentration resulted in the decrease of peak current. That's to say, the oxidation current of phenol changes abruptly around the critical micelles concentration (CMC) of CTAB [25]. Therefore, 1.3×10^{-4} mol/L CTAB was adopted as the optimum in this work.

The electrochemical oxidation of phenol compounds always involved proton transfer to form quinone [26]. Thus, the electrochemical response of phenol compounds can be affected by solution pH. From Figure 5C, it can be seen that the oxidation peak current gradually increases with an increasing pH value from 5.0 to 8.0. However, the oxidation peak current conversely decreased at the pH 9.0. In addition, the oxidation (E_{pa}) peak potentials shift negatively with increasing pH, indicating that the proton is directly involved in the electrochemical redox process of phenol [26]. Considering the determination sensitivity, the pH value of 8.0 was chosen as the optimal pH condition and used in the subsequent experiments.

3.5. Calibration curve

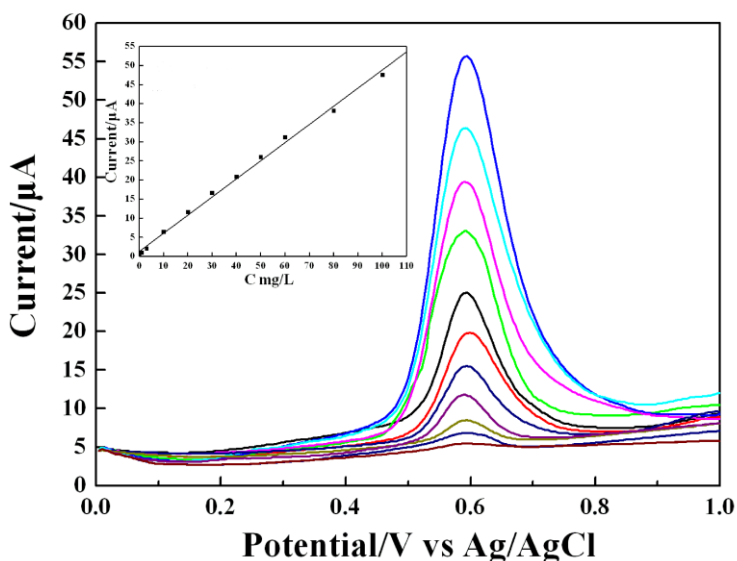


Figure 6. Differential pulse voltammograms of phenol of different concentrations ranging from 0.05 mg/L to 100 mg/L in 0.1 mol/L phosphate buffer (pH 8.0) at GR modified GCE in presence of 1.3×10^{-4} mol/L CTAB. The inset is the calibration curve of the oxidation peak current against the concentration of phenol.

DPV was performed to investigate the relationship between the peak current and concentration of phenol. As can be seen in Figure 6, under the optimal conditions, the oxidation peak current is proportional to phenol concentration in the range from 0.05 to 100 mg/L with the regression equation of $I_{pa} (\mu A) = 0.475C (mg/L) + 1.270 (R = 0.998)$. The detection limit was 0.02 mg/L ($S/N=3$). The wide linear range and the low detection limit can be attributed to the immobilization of graphene on the GCE surface with large surface area and excellent conductivity. The reproducibility of the GR-modified GCE was also examined by repetitive measurement of 50 mg/L phenol using the same GR-modified GCE in the presence of 1.3×10^{-4} mol/L CTAB. The relative standard deviation (RSD) for ten times measurement of 50 mg/L phenol was calculated to be 3.32%, indicating the good fabrication reproducibility.

3.6. Single factor experiment for phenol degradation

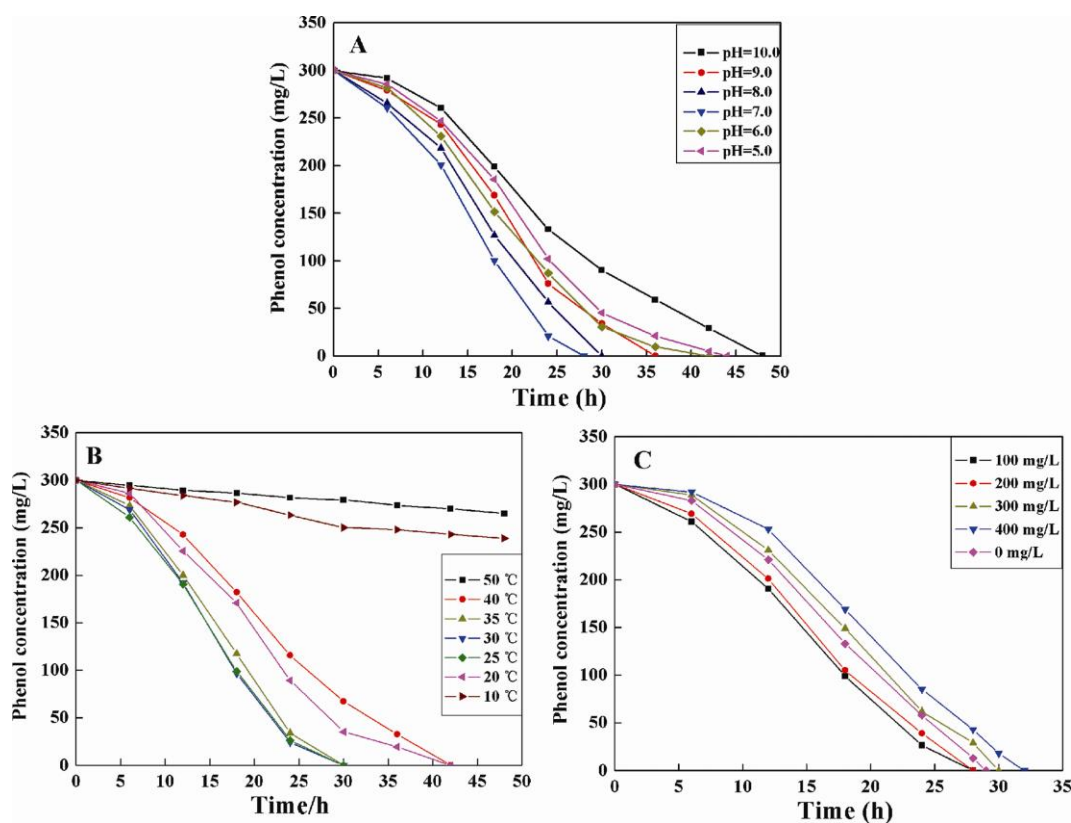


Figure 7. Phenol biodegradation at different initial pH values (A), temperatures (B) and glucose concentrations (C).

The medium pH is one of the significant factors in the success of the biological treatment process, which significantly affect the biochemical reactions required for phenol degradation. Most of the microorganisms cannot tolerate pH levels above 9.5 or below 4.0 [8]. However, the optimum pH for different microorganisms is different. Since high acidic environment and high basic environment increase the toxicity [27], the microbes grow efficiently at almost neutral medium. The concentration of phenol decreased with faster rate at pH of 7.0 as compared to other pH values (Figure 7A). But the

bacteria could also completely degrade phenol with longer time at other pH values. So, it can be inferred that *B. cereus* WJ1 can adapt over a wide pH range, indicating that WJ1 can be applied to different climates without altering the pH value. But extremely high or low pH values generally results in complete loss of activity for most of the enzymes [28]. These results support the statement that the growth rate of most organisms is usually maximum in the range of pH from 7.0 to 8.0 [29-31]. In conclusion, phenol degradation is deteriorated as the medium pH deviates from neutral condition. In the present work, the pH of medium was considered to be 7.0 for further degradation studies.

A variation of 5 °C may cause a decrease in phenol degradation rate of at least 50% at the lower end and almost 100% at the higher end. It can be seen from Figure 7B that the optimal value of temperature for phenol biodegradation is observed as 30 °C and phenol degradation rate at 25 and 35 °C are almost the same as 30 °C. The difference between phenol removal efficiency at 30 °C is probably due to the higher production of metabolites at this temperature [32]. The degradation rates dropped significantly with decreasing temperature lower than 20 °C and increasing temperature higher than 40 °C, indicating prominent inhibition of strain WJ1 at lower and higher temperature. Higher temperatures seemed to negatively affect the activity of the bacteria and hence hindered its biodegradation capabilities and even some bacteria were killed. On the other hand, exposure to lower temperatures was expected to slow down the bacterial activity. The results indicate that strain WJ1 grew slowly at 20 and 40 °C and nearly did not grow at 10 °C, while some of the bacteria dead at 50 °C. Moreover, earlier studies reported that most favorable temperature range for the phenol-degrading strain was 25-30 °C [4, 6, 33]. Thus, it is clear that the phenol degradation is temperature-dependent. The favorable temperature for the *B. cereus* WJ1 to degrade phenol is 30 °C.

The effect of additional glucose on phenol biodegraded by strain WJ1 was performed in the presence of different concentrations of glucose. The experimental results (Figure 7C) indicate that the rate of phenol removal was increased with low concentration of glucose (100 mg/L). This observation can be accounted for that glucose was the preferable substrate for degradation/metabolism, which can lead to a faster growth rate and higher biomass yield [34]. However, with the glucose concentration further increased, the degradation rate of phenol decreased and dropped below the rate achieved in the absence of glucose. That may be a result of catabolite repression by glucose, which has been observed by Wang et al. [35] that the presence of glucose can inhibit the utilization of the target substrate. Therefore, the presence of low concentration of glucose is beneficial for the phenol biodegradation.

3.7. Growth kinetic studies

In order to determine the growth kinetics, a series of batch experiments were conducted. The biodegradation of phenol and growth of strain WJ1 at different initial concentrations ranging from 50 to 600 mg/L are shown in Figure 8. The specific growth rates of the biomass μ under different initial phenol concentrations were calculated by Eq. (3). The yield coefficient was estimated by Eq. (5). Since the Haldane equation has been shown by several researchers [31, 33, 36] to give an adequate fit to plot of μ versus S , no other kinetic model was considered. Experimental and predicted specific growth rates of the culture due to Haldane's model are shown in Figure 9. The values of kinetic constants, μ_{\max} , K_s , K_i obtained in this work were $\mu_{\max}=0.153 \text{ h}^{-1}$, $K_s =21.33 \text{ mg/L}$ and $K_i =238 \text{ mg/L}$ ($R^2=0.969$),

respectively, and were compared with other published data in Table 2. It can be seen in Figure 9 that the value of specific growth rate increases with the increase in initial phenol concentration up to 100 mg/L, then it starts to decrease with further increase of phenol concentration.

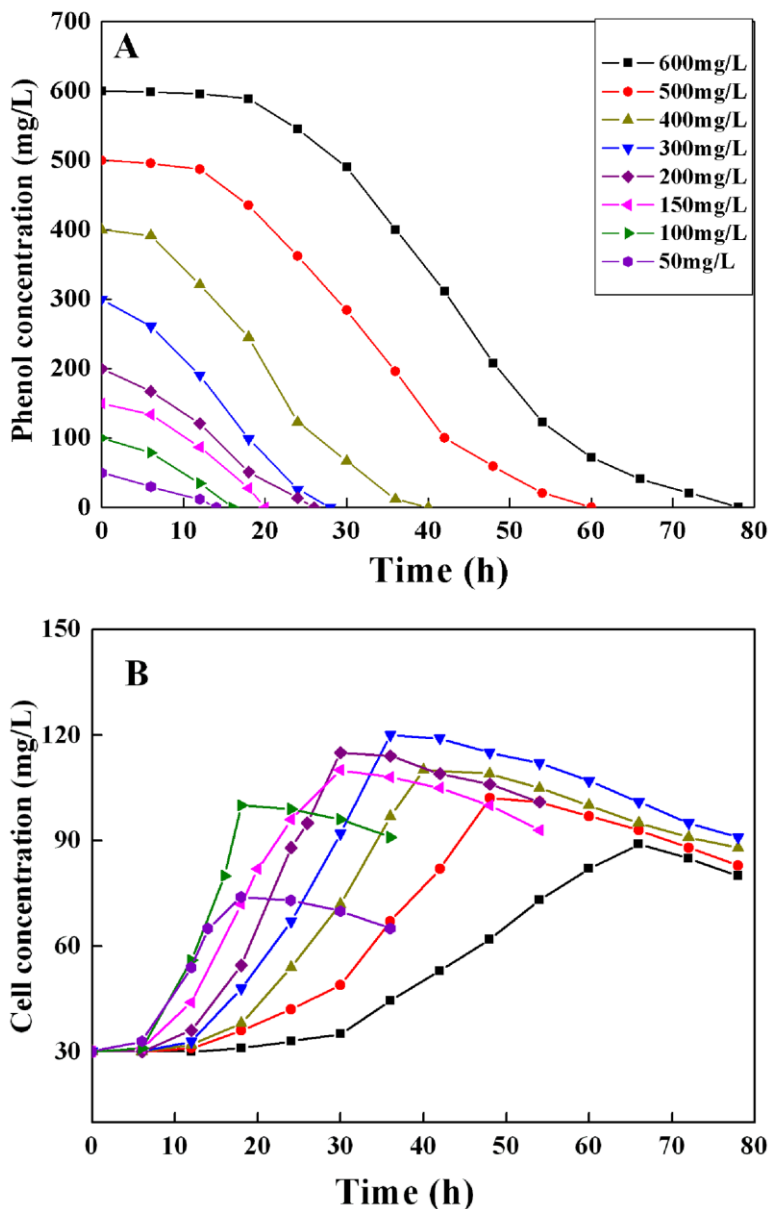


Figure 8. Biodegradation of phenol (A) and growth of the strain WJ1 (B) at different phenol concentrations.

The maximum specific growth rate occurred at low substrate concentration, which indicated that phenol was inhibitory type substrate and the inhibition effect of phenol became predominant above 100 mg/L. The small magnitude of K_s value indicates that for microbial species utilizing phenol, the maximum growth rate could be reached quickly, if the substrate inhibition has not been a factor [37].

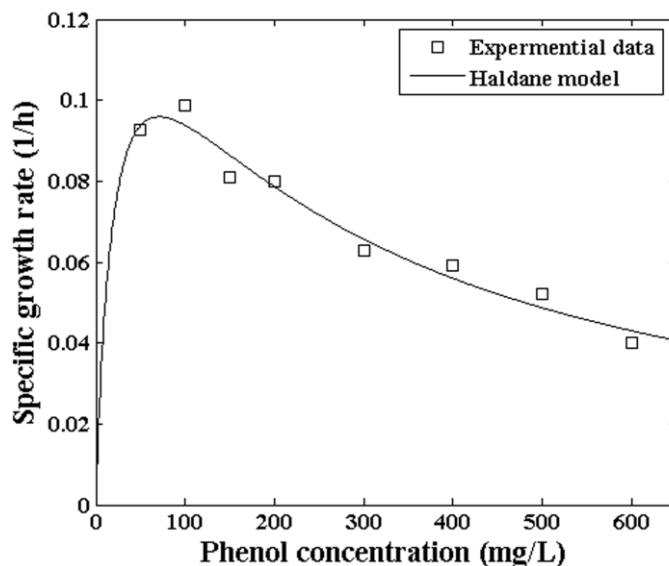


Figure 9. Kinetic prediction and experimental determined specific growth rate at initial phenol concentrations of 50-600 mg/L.

Table 2. Comparison of kinetic constant values in phenol degradation.

Culture	T (°C)	pH	Conc. Range (mg/L)	μ_{max} (1/h)	K_s (mg/L)	K_i (mg/L)	Reference
Yeast <i>Candida tropicalis</i>	30	6.8	250-1000	0.385	7.1	185	[4]
<i>Bacillus brevis</i>	34	8.0	750-1750	0.026	29.3	2434.7	[5]
<i>Corynebacterium</i> sp. DJ1	30	6.8-7.1	500-2500	0.656	33.1	1470	[6]
<i>Pseudomonas putida</i> LY1	25	7.1-7.3	20-380	0.217	24.4	121.7	[9]
<i>Bacillus cereus</i> MTCC 9818	37	7.5	0-2000	0.933	110.5	494.4	[28]
<i>Ewingella americana</i>	37	7.5	0-1000	0.29	5.16	1033.7	[29]
<i>Alcaligenes faecalis</i>	30	7.2	10-1400	0.150	2.22	245.4	[30]
Yeast <i>Candida tropicalis</i>	30	7.0	0-2000	0.48	11.7	208	[31]
Mixed culture	25	7.2	23.5-659	0.309	74.6	648.1	[33]
Mixed culture	25	6.5	500-3000	0.438	29.5	72.4	[37]
<i>Acinetobacter</i> sp.	30	7.4	60-350	0.80-0.85	1.2-1.5	188-315	[38]
<i>Bacillus cereus</i> WJ1	30	7.0	50-600	0.153	21.33	238	This work

From Eq. (5), it can be conclude that the initial phenol concentration was varied from 50 to 600 mg/L, to give a yield coefficient varying between 0.102 g/g and 0.880 g/g. This result is similar to that obtained by Li et al. [9], who found that the yield coefficient varied between 0.136 and 0.765 g/g as

initial phenol concentration varied from 20 to 380 mg/L. This phenomenon is based on the fact that the percentage of the total substrate carbon converted to energy for cell growth and maintenance increased as the specific growth rate decreased [39], when the inhibition effect of phenol became predominant above initial phenol concentration of 100 mg/L. More energy is required to overcome substrate inhibition effect during the phenol biodegradation. Therefore, substrate inhibition is not only to reduce the specific growth rate, but also to reduce the yield coefficient.

The decay coefficient k_d described the conversion of cell mass into maintenance energy and affected the growth kinetics because it appeared in the mass balance equation of the cell growth (Eq. (1)). During declining phase some parts of the cell population become food for the rest of the cell population. In order to determine the value of k_d , the growth of culture was continued and the cell mass concentration was observed for another 24 h even after the complete consumption of phenol. The slopes of all the curves during the in endogenous phase were in parallel, showing that the decay coefficient was not dependent on initial phenol concentration (Figure 8B). So, k_d was calculated according to Shen et al. [39] using an initial phenol concentration of 300 mg/L. The data of the endogenous region was plotted as a natural logarithm against time. The negative slope equated to the decay coefficient, which is 0.0066 h^{-1} . While, the decay rate coefficient values for *Pseudomonas putida* MTCC 1194 in phenol and catechol biodegradation system described by Kumar et al. [40] are 0.0056 h^{-1} and 0.0067 h^{-1} , respectively. The decay rate coefficient for *B. cereus* WJ1 in this study is similar to the reference mentioned above.

4. CONCLUSIONS

This work described the phenol biodegradation by using the bacterium *B. cereus* WJ1 which was isolated from a phenol-contaminated wastewater sample and identified on the basis of its morphological, biochemical characteristics and 16S rDNA sequence analysis. This bacterium grew well at pH 7.0 and 30 °C. Supplement of low concentration of glucose (100 mg/L) was helpful for accelerating the degradation of phenol. The kinetics of phenol biodegradation by *B. cereus* WJ1 was investigated at initial phenol concentrations ranging from 50 to 600 mg/L. The Haldane parameters for *B. cereus* WJ1 grown on phenol were obtained as $\mu_{\max} = 0.153 \text{ h}^{-1}$, $K_s = 21.33 \text{ mg/L}$ and $K_i = 238 \text{ mg/L}$. Combining the unique properties of graphene, such as high specific surface area and excellent conductivity with synergistic adsorption of CTAB onto the electrode surface, the GR-CTAB/GCE resulted in remarkable peak current enhancement of phenol. Therefore, the fabricated electrode can be applied to the determination of phenol concentration in water samples.

ACKNOWLEDGEMENTS

This work is supported by the National Natural Science Foundation of China under Grant Nos. 20577017 and 41161080.

References

1. K. Bandhyopadhyay, D. Das, P. Bhattacharyya, B.R. Maiti, *Biochem. Eng. J.* 8 (2001) 179.

2. M. Mollaei, S. Abdollahpoura, S. Atashgahi, H. Abbasi, F. Masoomi, I. Rada, A.S. Lotfi, H.S. Zahiri, H. Vali, K.A. Noghabi, *J. Hazard. Mater.* 175 (2010) 284.
3. R.N. Singh, D. Mishra, Anindita, *Int. J. Electrochem. Sci.* 4 (2009) 1638.
4. S.S. Adav, M.Y. Chen, D.J. Lee, N.Q. Ren, *Biotechnol. Bioeng.* 96 (2007) 844.
5. V. Arutchelvan, V. Kanakasabai, R. Elangovan, S. Nagarajan, V. Muralikrishnan, *J. Hazard. Mater.* B129 (2006) 216.
6. K.L. Ho, B. Lin, Y.Y. Chen, D.J. Lee, *Bioresour. Technol.* 100 (2009) 5051.
7. D.B. Lu, Y. Zhang, S.Q. Niu, L.T. Wang, S.X. Lin, C.M. Wang, W.C. Ye, C.L. Yan, *Biodegradation* 23 (2012) 209.
8. R.K. Singh, S. Kumar, S. Kumar, A. Kumar, *Biochem. Eng. J.* 40 (2008) 293.
9. Y. Li, J. Li, C. Wang, P.F. Wang, *Bioresour. Technol.* 101 (2010) 6740.
10. E. Ballesteros, M. Gallego, M. Valcárcel, *J. Chromatogr. A* 518 (1990) 59.
11. R. Belloli, B. Barletta, E. Bolzacchini, S. Meinardi, M. Orlandi, B. Rindone, *J. Chromatogr. A* 846 (1999) 277.
12. W. Frenzel, S. Krekler, *Anal. Chim. Acta* 310 (1995) 437.
13. S.V. Dzyadevych, T.M. Anh, A.P. Soldatkin, N.D. Chien, N.J. Renault, J.M. Chovelon, *Bioelectrochemistry* 55 (2002) 79.
14. G. Wang, J.J. Xu, L.H. Ye, J.J. Zhu, H.Y. Chen, *Bioelectrochemistry* 57 (2002) 33.
15. T. Ndlovu, O.A. Arotiba, R.W. Krause, B.B. Mamba, *Int. J. Electrochem. Sci.* 5 (2010) 1179.
16. Y. Wang, Y.M. Li, L.H. Tang, J. Lu, J.H. Li, *Electrochem. Commun.* 11 (2009) 889.
17. C.S. Shan, H.F. Yang, D.X. Han, Q.X. Zhang, A. Ivaska, L. Niu, *Biosens. Bioelectron.* 25 (2010) 1070.
18. Z.J. Zhuang, J.Y. Li, R. Xu, D. Xiao, *Int. J. Electrochem. Sci.* 6 (2011) 2149.
19. J.F. Rusling, *Acc. Chem. Res.* 24 (1991) 75.
20. W.S. Hummers, R.E. Offeman, *J. Am. Chem. Soc.* 80 (1958) 1339.
21. X. Fan, W. Peng, Y. Li, X. Li, S. Wang, G. Zhang, F. Zhang, *Adv. Mater.* 20 (2008) 4490.
22. M.Y. Chao, X.Y. Ma, X. Li, *Int. J. Electrochem. Sci.* 7 (2012) 2201.
23. D.B. Lu, S.X. Lin, L.T. Wang, X.Z. Shi, C.M. Wang, Y. Zhang, *Electrochim. Acta* 85 (2012) 131.
24. Y. Wang, Y.M. Li, L.H. Tang, J. Lu, J.H. Li, *Electrochem. Commun.* 11 (2009) 889.
25. Y. Peng, J.H. Xu, J. Zhao, B.L. Hu, S.S. Hu, *Russ. J. Electrochem.* 44 (2008) 222.
26. X.Y. Li, Y.H. Cui, Y.J. Feng, Z.M. Xie, J.D. Gu, *Water Res.* 39 (2005) 1972.
27. M. Kulkarni, A. Chaudhari, *Bioresour. Technol.* 97 (2006) 982.
28. Banerjee, A.K. Ghoshal, *J. Hazard. Mater.* 176 (2010) 85.
29. K.M. Khleifat, *Process Biochem.* 41 (2006) 2010.
30. J. Bai, J.P. Wen, H.M. Li, Y. Jiang, *Process Biochem.* 42 (2007) 510.
31. Y. Jiang, J.P. Wen, J. Bai, D.Q. Wang, Z.D. Hu, *Biochem. Eng. J.* 29 (2006) 227.
32. C.S.A. Sá, R.A.R. Boaventura, *Biochem. Eng. J.* 9 (2001) 211.
33. M. Bajaj, C. Gallert, J. Winter, *Biochem. Eng. J.* 46 (2009) 205.
34. K.C. Lob, C. P.P. Tar, *Bull. Environ. Contam. Toxicol.* 64 (2000) 756.
35. K.W. Wang, B. C. Baltzis, G. A. Lewandowski, *Biotechnol. Bioeng.* 51 (1996) 87.
36. C.L. Zheng, J.T. Zhou, J. Wang, J. Wang, B.C. Qu, *J. Hazard. Mater.* 160 (2008) 194.
37. B. Marrot, A. Barrios-Martinez, P. Moulin, N. Roche, *Biochem. Eng. J.* 30 (2006) 174.
38. J. Hao, M. H. Kim, E. A. Seagren, H. Kim, *Chemosphere* 46 (2002) 797.
39. J.Y. Shen, R. He, L.J. Wang, J.F. Zhang, Y. Zuo, Y.C. Li, X.Y. Sun, J.S. Li, W.Q. Han, *J. Hazard. Mater.* 167 (2009) 193.
40. Kumar, S. Kumar, S. Kumar, *Biochem. Eng. J.* 22 (2005) 151.